Journal of Rock Mechanics and Geotechnical Engineering xxx (xxxx) xxx

Contents lists available at ScienceDirect

Journal of Rock Mechanics and Geotechnical Engineering

journal homepage: www.jrmge.cn

Full Length Article

Numerical parametric study on the influence of location and inclination of large-scale asperities on the shear strength of concrete-rock interfaces of small buttress dams

Dipen Bista [a, b, *], Adrian Ulfberg [c], Leif Lia [b], Jaime Gonzalez-Libreros [c], Fredrik Johansson [d], Gabriel Sas [c]

[a] Sintef Narvik AS, 8517, Narvik, Norway
[b] Norwegian University of Science and Technology (NTNU), 7491, Trondheim, Norway
[c] Luleå University of Technology (LTU), 97187, Luleå, Sweden
[d] KTH Royal Institute of Technology, 10044, Stockholm, Sweden

ARTICLE INFO

Article history:
Received 10 August 2023
Received in revised form
21 October 2023
Accepted 4 December 2023

Keywords:
Concrete dam
Buttress dam
Sliding
Shear strength
Concrete-rock interface
Asperity inclination
Asperity location

ABSTRACT

When assessing the sliding stability of a concrete dam, the influence of large-scale asperities in the sliding plane is often ignored due to limitations of the analytical rigid body assessment methods provided by current dam assessment guidelines. However, these asperities can potentially improve the load capacity of a concrete dam in terms of sliding stability. Although their influence in a sliding plane has been thoroughly studied for direct shear, their influence under eccentric loading, as in the case of dams, is unknown. This paper presents the results of a parametric study that used finite element analysis (FEA) to investigate the influence of large-scale asperities on the load capacity of small buttress dams. By varying the inclination and location of an asperity located in the concrete-rock interface along with the strength of the rock foundation material, transitions between different failure modes and correlations between the load capacity and the varied parameters were observed. The results indicated that the inclination of the asperity had a significant impact on the failure mode. When the inclination was 30° and greater, interlocking occurred between the dam and foundation and the governing failure modes were either rupture of the dam body or asperity. When the asperity inclination was significant enough to provide interlocking, the load capacity of the dam was impacted by the strength of the rock in the foundation through influencing the load capacity of the asperity. The location of the asperity along the concrete-rock interface did not affect the failure mode, except for when the asperity was located at the toe of the dam, but had an influence on the load capacity when the failure occurred by rupture of the buttress or by sliding. By accounting for a single large-scale asperity in the concrete-rock interface of the analysed dam, a horizontal load capacity increase of 30%–160% was obtained, depending on the inclination and location of the asperity and the strength of the foundation material.

1. Introduction

In stability assessments of concrete gravity or buttress dams, sliding failure is one of the modes of failure for which the dam must meet recommended safety requirements (NVE, 2005; USACE, 1976; CFBR, 2012). Sliding failure is horizontal displacement of a section or the whole dam along a failure plane, and the safety against such a failure is conventionally defined by a safety factor. The safety factor for sliding failure is determined by comparing the shear forces acting on potential failure planes and the planes' shear capacity (ICOLD, 2004; NVE, 2005; CFBR, 2012). Several potential failure planes may exist in a dam and its foundation, such as in the construction joints of the dam, the concrete-rock interface, and sub-horizontal rock joints in the dam foundation (CFBR, 2012).

Sliding safety assessment is often carried out analytically, as

* Corresponding author. Sintef Narvik AS, 8517, Narvik, Norway.
E-mail address: dipen.bista@ntnu.no (D. Bista).

Peer review under responsibility of Institute of Rock and Soil Mechanics, Chinese Academy of Sciences.

https://doi.org/10.1016/j.jrmge.2023.12.036

Please cite this article as: D. Bista, A. Ulfberg, L. Lia *et al.*, Numerical parametric study on the influence of location and inclination of large-scale asperities on the shear strength of concrete-rock interfaces of small buttress dams, Journal of Rock Mechanics and Geotechnical Engineering, https://doi.org/10.1016/j.jrmge.2023.12.036

commonly prescribed by regulatory rules and guidelines (ANCOLD, 1991; NVE, 2005; USACE, 1976; CFBR, 2012; FERC, 2016), in which the geometry of a failure plane is inferred. The sections of the dam and/or foundation on each side of the failure plane are assumed to be rigid bodies. The shear strength of the failure plane is normally estimated using the Mohr-Coulomb (MC) failure criterion (ANCOLD, 1991; NVE, 2005; USACE, 1976; CFBR, 2012; FERC, 2016). The MC failure criterion employs three parameters to approximate the shear strength of an interface (i.e. failure plane), i.e. the friction angle, the normal stress acting on the interface, and cohesion. There are usually large uncertainties related to cohesion and it is thus often ignored in dam assessment (Westberg Wilde and Johansson, 2016). The friction angle is normally obtained from laboratory or in situ tests, or from recommended values in the guidelines (Bista et al., 2020). The normal stress and the shear stress acting on the potential failure plane are assumed to be constant over its entire area and are computed based on the loads acting on the dam.

By virtue of the aforementioned assumptions, the failure plane with the lowest safety factor (i.e. governing) employed by the analytical rigid body methods may not accurately trace the weak planes, e.g. the concrete-rock interface or the constructions joints in the dam. Furthermore, only force equilibrium is considered and any potential stress redistribution, due to small displacements along an irregular failure plane, is not considered (USACE, 1976). The governing failure plane may also intersect solid (i.e. non-fractured) portions of intact rock and concrete.

However, a dam foundation surface is normally prepared by blasting and cleaning the top surface to remove weak and weathered rock (Zhang et al., 2013). Therefore, the foundation profile often contains irregularities, i.e. large-scale asperities (at the decimetre or metre scale). An example of a foundation profile of a section in an existing Norwegian dam, the Kalhovd dam, is presented in Fig. 1a (Bista et al., 2020). Fig. 1b and c shows the distribution of the inclination and size of the large-scale asperities at the Kalhovd dam. Due to the difference in scale between laboratory samples and the large-scale asperities in a dam, parameters for the MC criterion, obtained from laboratory, do not usually consider the effect of large-scale asperities (Bandis et al., 1981; Hencher et al., 1993). However, research has shown that the overall shear strength of the failure plane is determined by the presence of large-scale asperities (Patton, 1966; Grasselli, 2001; Asadi et al., 2013; Zhang et al., 2016).

Hence, analytic evaluation of the sliding safety of the concrete-rock interface of a dam that contains large-scale asperities suffers from potential shortcomings, mainly due to the assumption and idealisation of the geometry of the failure plane and the uncertainty in quantifying its shear strength.

Although the effect of large-scale asperities has been thoroughly studied for interfaces (i.e. failure plane) of simple bodies under direct shear (Patton, 1966; Grasselli, 2001; Zhang et al., 2016), only a few studies have investigated their impact on the load capacity of dams. The results of tests on small-scale samples by Bista et al. (2020) and a scale model test by Sas et al. (2021) showed that, in addition to sliding, the presence of large-scale asperities in the concrete-rock interface may also lead to failure due to rupture of the dam body and shearing of the asperity. Such types of failures are not typically considered in analytical assessment of a dam. Furthermore, in the scale model test by Sas et al. (2021), the shear strength of a scale model with a large-scale asperity was up to 10 times that of a scale model without any asperities (referred to as the reference model). The concrete-rock interface for the reference model in the study by Sas et al. (2021) had the geometry of a typically chosen failure plane for sliding. The significant difference between the capacities of the scale models suggests that large-scale asperities may substantially influence the load capacity of a dam.

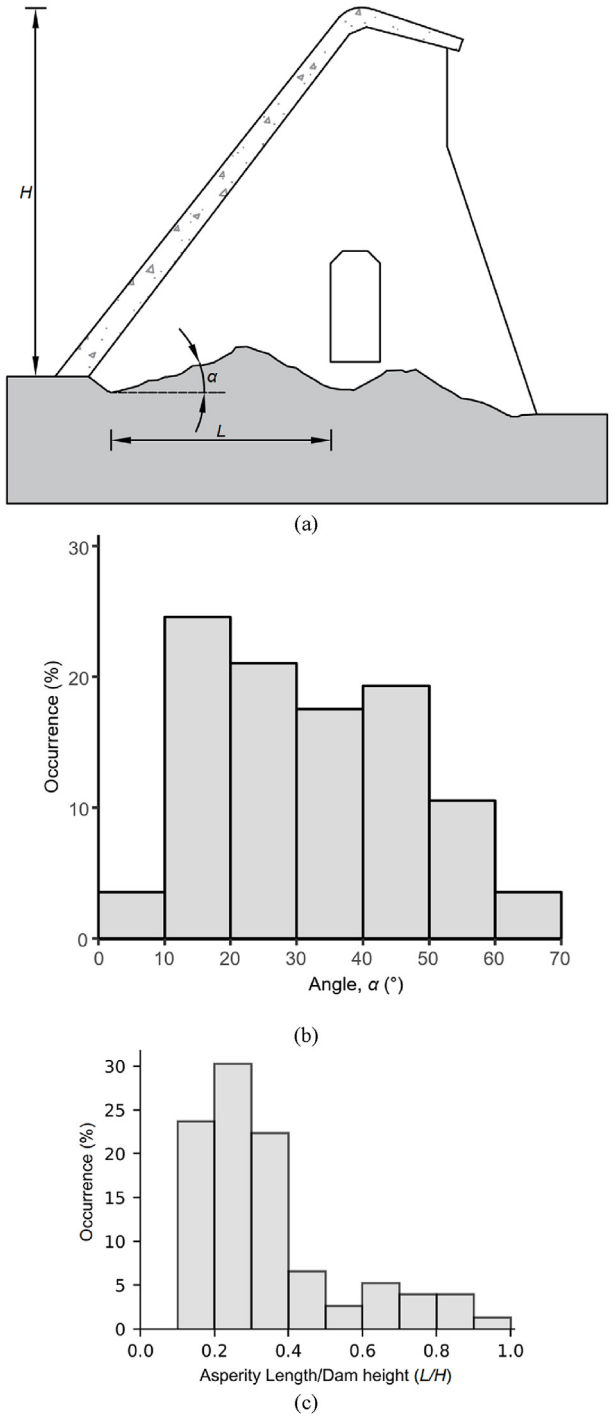

Fig. 1. (a) Profile of the rock foundation for a section in the Kalhovd dam in Norway, (b) distribution of the inclinations of the large-scale asperities in the rock foundation of Kalhovd dam in Norway (Bista et al., 2020), and (c) distribution of the size of the asperities in the foundation profile of Kalhovd dam in Norway, expressed as a ratio of asperity length to dam height. Reproduced under the terms of the Creative Commons Attribution (CC BY-NC-ND 4.0) license.

Studies by Kodikara and Johnston (1994), Liahagen et al. (2012), Johansson and Stille (2014), Bista et al. (2020) and Sas et al. (2021) have shown that the failure of a sheared interface is heavily dependent on the inclination of large-scale asperities. Sliding only occurs for sheared interfaces where the large-scale asperities have low inclinations (about 30° and less), while asperities with large

inclinations prevent sliding and act as shear keys. Hence, for dams with asperities with large inclinations in the concrete-rock interface, failures such as rupture of the dam body or shearing of the asperity could potentially be more likely than sliding.

Furthermore, Bista et al. (2020) investigated the influence of the location of a single asperity along the sheared interface in laboratory tests. In these tests, it was shown that the failure mode, and hence the shear strength of the interface, was dependent on the location of the asperity. This effect was due to the asperity's influence on the stress distribution along the interface giving rise to stress concentrations. Similarly, stress concentrations caused by large-scale asperities were also evident in the scale model tests by Sas et al. (2021).

While large-scale asperities have been proven to influence the load capacity and behaviour of sheared interfaces under direct shear, few studies have investigated their effect under eccentric loading conditions, as in the case of dams. Additionally, the influence of an asperity's inclination and location on the sheared interface's load capacity has only been evaluated for simple sections/bodies in contact under rudimentary loading conditions. Therefore, using finite element analysis (FEA), this study investigated the influence of the inclination and location of a large-scale asperity present in the concrete-rock interface on a dam's load capacity. It is hypothesised that an asperity that is identifiable on-site and that possesses sufficient strength to withstand the hydrostatic load exerted by the dam on its own, without experiencing failure, could be considered a large-scale asperity. By using several different configurations of a single large-scale asperity's inclination and location in the interface of a concrete buttress dam, different failure modes and capacities were obtained and are discussed along with the implication of the study's result on dam safety.

2. Design of experiment

In this study, 84 different finite element (FE) models were created to evaluate the horizontal load capacity of a dam with a single large-scale asperity with seven different inclinations, at four different locations along the concrete-rock interface, with three different sets of material parameters. A reference model without an asperity in the interface was also created. The reference model was geometrically equivalent to that employed by common analytical rigid body methods, where the geometry of the concrete-rock interface is idealised and large-scale asperities are ignored.

The geometry and dimensions of the buttress dam in this study are based on a typical Norwegian flat slab buttress dam with a height of 6 m. A flat slab buttress dam has a continuous plate, referred to as the front plate, which acts as the impermeable boundary for the water in the reservoir. The front plate is supported at regular intervals by buttresses. For a 6 m tall buttress dam, the buttresses are usually spaced at 5 m. The theoretical basis for this type of dam design is that each individual buttress supports a 5 m segment of the front plate. Dam Langesæ, located in Vinje municipality in Norway and depicted in Fig. 2, is a flat slab buttress dam.

To investigate the influence of the inclination of a large-scale asperity on the load capacity of the dam, and at which inclination the failure mode of the dam changes, inclinations between 15° and 45° (in increments of 5°) were chosen for the large-scale asperity in this study. As natural asperities lack a distinct geometrical shape, they have frequently been approximated as triangular, trapezoidal, or sinusoidal waveforms for analysis purposes (e.g. Kodikara and Johnston, 1994; Grasselli, 2006; Andjelkovic et al., 2015). Numerical singularities in a FE model tend to occur at a point of stress concentration, typically at sharp re-entrant corners in the mesh. Hence, a trapezoidal shape of the asperity was chosen where the top length of the trapezoid was 20% of the base length. An asperity length equal to 10% of the dam's height was chosen for the models, corresponding to a 60 cm long asperity in the FE models. The chosen size of the asperity was based on the assumption that a large-scale asperity would be identifiable on-site and large enough to be able to withstand the load exerted from the hydrostatic pressure on the dam.

Four different locations of asperity were analysed to study the influence of the location of the asperity along the concrete-rock interface. The asperity was placed at 25%, 50%, 75% and 100% (dam toe), relative to the dam's length measured from its heel. The asperity geometry, dimensions, and locations in the concrete-rock interface are depicted in Fig. 3.

Three different loads were considered in the study: (1) the self-weight of the dam, (2) hydrostatic pressure from the water (with the water level at the crest of the dam), and (3) the horizontal component of the hydrostatic pressure. First, the self-weight of the dam and the hydrostatic pressure (both the vertical and horizontal components) were applied. Subsequently, the horizontal component of the hydrostatic pressure was applied until failure of the FE models. The reasoning behind only applying the horizontal component of the hydrostatic pressure until failure was to induce failure of the models without further increasing the normal stresses in the concrete-rock interface, as heightened normal stresses would increase the shear capacity of the interface even further.

The dam in this study has a relatively thin front plate and buttresses. Consequently, the uplift force on the front plate would be relatively small while the buttresses are drained on both sides. Therefore, the uplift force was ignored due to the relatively small force magnitudes.

3. Finite element models

The FEA software used for the study was ATENA Science v5 (Červenka et al., 2021). All FEA models in the study were constructed in two-dimensional (2D) and were composed of several different element and material models. A single free-standing buttress dam monolith (i.e. a portion of the front plate with a single buttress) was analysed. Each model was comprised of a 5 m segment of the front plate, buttress, foundation, asperity, interface, and a linear elastic material. Nonlinear material models were used in the study to permit cracking as well as to allow for dry friction and separation of the interface. Interaction effects exist between monoliths for certain dams with shear keys in the expansion joints (Enzell, 2023). However, these effects are currently not quantifiable and not all dams are constructed with shear keys in the joints between the monoliths. Consequently, any interaction effect between the monoliths was ignored.

3.1. Geometry and material models

Only the inclination and location of the asperity and the strength of the foundation differs between the 85 models in the study. An overview of the FEA model with asperity at 100%, relative to the dam's length measured from the heel, is presented in Fig. 4 and the input parameters used for the materials used throughout the study given in Tables 1 and 2.

3.1.1. Concrete, foundation, and linear elastic material

The buttress of a typical Norwegian flat slab buttress dam has a variable thickness along its height. For a height of 6 m, the buttress is typically 300 mm thick at the top and increases in thickness by 25 mm for every vertical metre towards the bottom (Sas et al., 2015). As a 2D model was employed, the resulting average thickness of 0.375 m for the fictitious dam buttress was chosen as the thickness in the model. The asperity in each model was given the

Fig. 2. Photo of Dam Langesæ located in Vinje municipality in Norway (Provided by Statkraft).

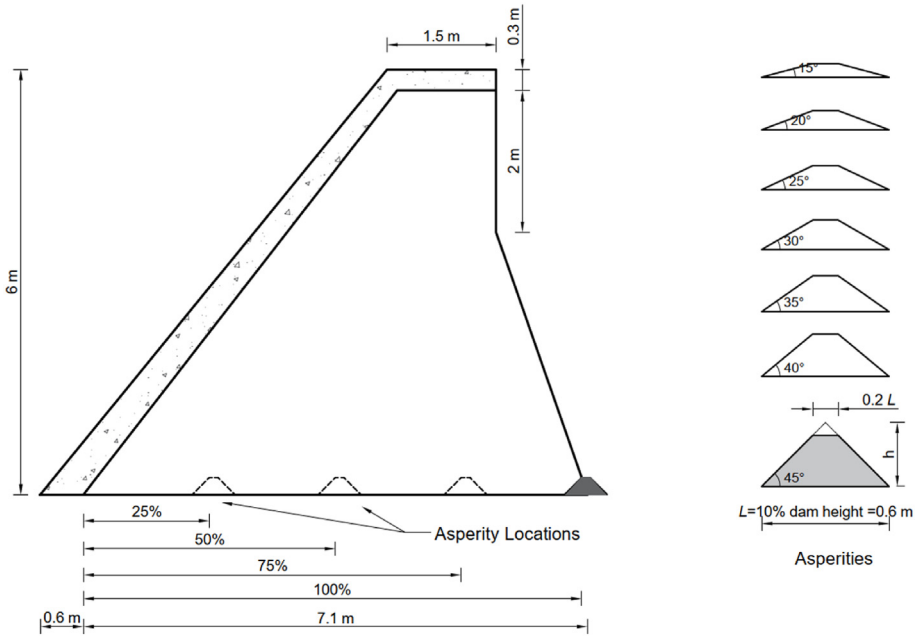

Fig. 3. Geometry of dam and asperities used in the FE models.

same thickness and both the buttress and the asperity employed plane stress idealisation.

For the buttress dam type used in this study, buttresses individually support a section of the front plate. A flat slab buttress dam of this size often supports a section of 5 m of the front plate (Sas et al., 2015). Consequently, the thickness of the front plate was set to 5 m in the FEA models. Similarly, the foundation was also given a thickness of 5 m. Both the front plate and the foundation were given plane strain idealisation. To truncate the geometrical size of the model and to prevent erroneous cracking of the foundation due to stress concentrations from nodal supports, a linear elastic material was added to the FEA model at the boundaries of the foundation. Consequently, the foundation was modelled with a depth of 3 m and extended 2 m from the dam's toe and heel. The linear elastic material was modelled using plane strain elements and had material parameters corresponding to those of structural steel.

The front plate, buttress, foundation, and asperity were created with a material model named "Cementitious2" which is a fracture-plastic material model in ATENA v5 (Červenka et al., 2021). This material model employs the Rankine failure criterion and exponential tension softening along with an orthotropic smeared crack model (Červenka et al., 2021). Four different sets of inputs were used for this material model to create the "concrete" and "foundation" (with compressive strengths of 50 MPa, 100 MPa, and 150 MPa, based on Hoek and Brown (1997)).

The concrete material, used for the buttress and front plate, was generated using the parameter relationships given in Eurocode 2 (EN 1992-1-1, 2004). The concrete corresponded to a C30/37 concrete where the mean value of 38 MPa was used as the cylindrical

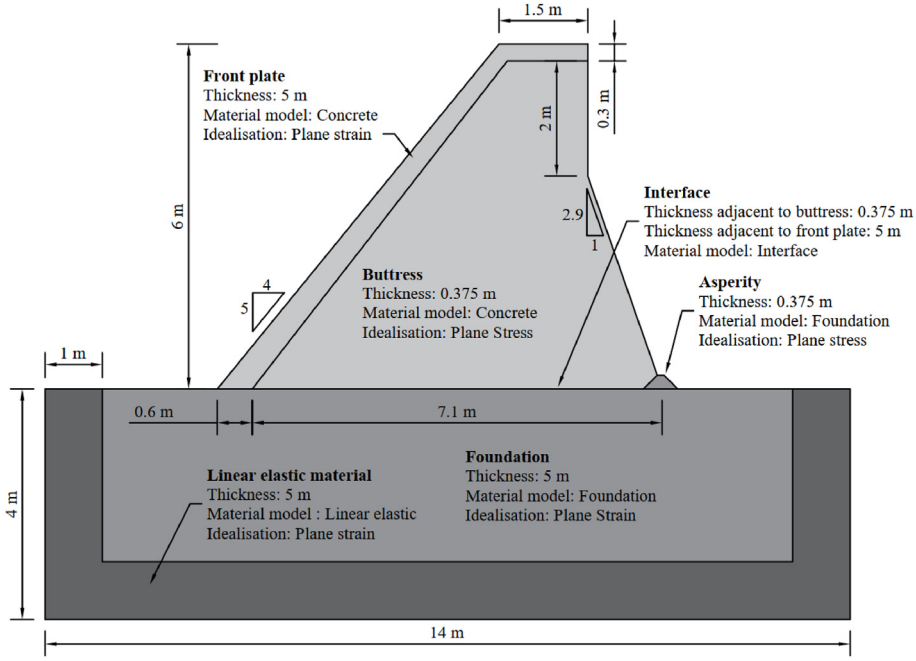

Fig. 4. Overview of FEA model with the asperity at 100%, relative to the dam's length measured from the heel.

Table 1
Material properties used in the FE models.

Material mode		σ_c (MPa)	σ_t (MPa)	E (GPa)	ν	G_f (N/m)	ε_c^p	σ_{c0} (MPa)	r_c	W_d (mm)
Foundation	$\sigma_c = 150$ MPa	150	6	50	0.2	188.8	−38	15.9	0.8	−0.5
	$\sigma_c = 100$ MPa	100	5	44	0.2	125	−71	10.5	0.8	−0.5
	$\sigma_c = 50$ MPa	50	3.8	36	0.2	95	−96	8	0.8	−0.5
Concrete		38	2.9	32	0.2	72.5	−101	6.1	0.8	−0.5
Elastic material		–	–	200	0.3	–	–	–	–	–

Note: σ_c is the compressive strength, σ_t is the tensile strength, E is the Young's modulus, ν is the Poisson's ratio, G_f is the fracture energy, ε_c^p is the plastic strain at cylindrical compressive strength, σ_{c0} is the compressive stress at onset of crushing, r_c is the compressive strength reduction due to cracking, and W_d is the critical compressive displacement.

Table 2
Mechanical properties of the concrete-rock interface.

Property	Unit	Value
Normal stiffness	MN/m^3	3.2×10^6
Tangential stiffness	MN/m^3	1.3×10^6
Cohesion	kPa	0.1
Tension strength	kPa	0.1
Friction coefficient		0.7
Minimal normal stiffness	MN/m^3	3200
Minimal tangential stiffness	MN/m^3	1333.3

compressive strength in the concrete material model. A similar value of the mean compressive strength of concrete was reported in tests of existing dams (Sas et al., 2021). For this study, the rock (i.e. foundation material) was assumed to be intact. Few research studies were found on the tensile region of the stress-strain curve for intact rock. Furthermore, the tensile strength of the intact rock exhibits large variations (Perras and Diederichs, 2014). Since rock, as a material, experiences both compressive and tensile softening (Perras and Diederichs, 2014; Wu et al., 2018), a concrete material model was considered to be able to represent the stress-strain behaviour of the rock. As a fictitious dam was used for this study and no data from material tests were readily available, the tensile strength and other related model parameters were extrapolated from the parameter relationship given in the Eurocode 2 (EN 1992-1-1, 2004). For strong and very strong intact rocks, the ratio between the tensile strength and compressive strength is potentially greater than those used for this study (Perras and Diederichs, 2014; Briševac et al., 2015). Consequently, the load capacity for the models which experienced material failure could be conservative. However, the influence of inclination, location, and material strength of the asperity can still be captured.

3.1.2. Interface

The interface elements utilised in the study consisted of two hyperplanes (i.e. lines in 2D analyses) with each connected to each body in contact. The penalty method was used for interface elements with two different states possible; the elements could either be in an open or a closed state (Červenka et al., 2021). The closed state refers to full interaction (i.e. contact) between the adjoined bodies whereas the open state refers to no interaction between them (i.e. separation). The stresses in the interface element in relation to the tension strength in the interface material model determine the state of the interface elements. The stiffness of the interface elements depends on the state. Consequently, four different parameters (for a 2D analysis) were defined to describe the interface elements' normal and tangential stiffness, in each state. Note that interface stiffness is only a parameter that exists for numerical purposes.

The interface elements can be viewed as springs with a

nonlinear stiffness, connecting the bodies in contact. Interface elements will deform during the analysis and too low stiffness may potentially postpone cracking (Pryl and Červenka, 2018). It is therefore necessary for the interface elements to be sufficiently stiff. However, too high interface stiffness may lead to convergence issues. Hence, a sensitivity analysis was carried out on the models to determine an appropriate interface stiffness. The sensitivity analysis showed that the interface stiffness chosen for this study generated similar results to that of an interface that was 10 times stiffer, implying that the chosen interface stiffness was still sufficiently stiff, while having greater numerical stability. The interface stiffness parameters chosen for this study are given in Table 2 and are equivalent to the stiffness of an element in the concrete dam near the interface. In the closed state, the interface can thus be interpreted as having a fictional thickness of 1 cm and a Young's modulus equal to that of the concrete.

The interface material model was based on the MC failure criterion but replaced the tension side of the criterion with an ellipsoid, defined by cohesion and a tension strength parameter (Červenka et al., 2021). The input parameters used for the interface material models are summarised in Table 1. Normal stiffness and the tangential stiffness in Table 2 refer to the interface's stiffness in the closed state whereas the minimal normal stiffness and minimal tangential stiffness refer to the open state. Realistically, the stiffness should be zero for the open state. However, for numerical stability, it is recommended that the stiffness in the open state is at least one thousandth of the stiffness in the closed state (Červenka et al., 2021). The friction angle was assumed to have a mean value of 35°, which corresponds to a friction coefficient of 0.7 (EPRI, 1992; Westberg Wilde and Johansson, 2016). Cohesion was not intended to be included in the analysis due to the large uncertainties related to cohesion (Westberg Wilde and Johansson, 2016) and is therefore often ignored in dam assessment. However, the interface cohesion and tension strength were chosen to be 0.1 kPa in the analyses, as non-zero magnitudes for the tensile strength and cohesion are recommended for numerical stability (Červenka et al., 2021).

3.1.3. Mesh

A mesh sensitivity analysis was carried out on the models before the study. The mesh sensitivity analysis showed that the load capacity converged within 2% for the models with a mesh size between 0.01 and 0.03 m for the elements at the interface, and 0.1–0.3 m for the elements in the dam body and foundation. Consequently, the mesh size chosen for the models was 0.01 m for the elements at the interface and 0.1 m for the dam body.

3.2. Loads and boundary conditions

Loads were applied as forces to the model. Three different loads were applied to the models in the analyses, i.e. the self-weight of the dam, hydrostatic pressure corresponding to water up to the top of the dam (highest regulated water level), and the horizontal component of hydrostatic pressure. The order in which they were applied, and the number of load steps implemented for each are described in Section 3.4. Four nodal supports, connected to the linear elastic material, were used as boundary conditions for the models. The reason behind using nodal supports, instead of continuous supports along the boundary lines of the linear elastic material, was so that the reactions could be easily verified against the applied loads. Fig. 5 shows a graphical depiction of the loads.

3.3. Analysis procedure and convergence criteria

The first 120 load steps applied the self-weight of the dam. Consecutively, the hydrostatic pressure was applied to the models over next 130 load steps. Last, from load step 250, the horizontal component of the hydrostatic pressure was applied, with no defined number of load steps, but was instead applied in load steps of 0.5% (of the full horizontal component hydrostatic load) until the models reached failure. Newton-Raphson was chosen as the solution method and was given a maximum iteration limit of 200.

For a step to converge, the maximum residual error allowed for at the end of a load step was 0.1% for displacements and forces, whereas the tolerance for energy was set to 0.01%. The conditional break criterion was set to a maximum error of 1% at the end of a load step, for any of the aforementioned residual errors, meaning that the analyses were immediately terminated in the case of exceedance at the end of a load step. Note that a non-converged load step did not result in immediate termination of the analysis and was allowed to progress even after a diverged step unless the conditional break criteria were violated.

Failure was deemed to have occurred when the solver did not converge for two consecutive load steps or if the conditional break criterion was violated. The reasoning behind this failure criteria is the fact that the convergence criteria were strict but considered necessary to allow for an accurate comparison of such nonlinear models that exhibited different types of failures. It should be mentioned that the emergence and propagation of cracks may result in a non-converged load step. However, the maximum total number of non-converged load steps seen for any of the 85 analyses ran (before the violation of the failure criteria) was six, all with less than 1% residual error. The average number of load steps applied in the models before the failure criteria was violated was 443.

4. Results

The results of the FEA model simulations showed that, depending on the inclination of the asperity, an interlocking effect was produced which changed the stress flow in the dam hence inducing a failure either in the concrete of the buttress or at the asperity. Hence, the models failed in three different ways: by sliding, by cracking of concrete in the buttress (i.e. buttress failure), or by shearing of the asperity (i.e. asperity failure). These obtained failure modes, and the behaviour of the dam leading up to failure for each failure mode, mirror the results from the physical experiments by Bista et al. (2020) and Sas et al. (2021). However, it is not possible to draw any conclusions concerning the load capacities obtained from the models in the study due to dissimilar loading schemes and concrete-rock interface geometries.

For some models, especially the ones with an asperity at the 25%, 50% and 75% locations, a combined sliding and rotation was observed. Similar behaviour of the samples was also reported by Bista et al. (2020) and Sas et al. (2021). Such behaviour was expected due to the interlocking effect and stress concentration at the asperity and the eccentric nature of the hydrostatic load applied. For these models, the part of the buttress dam in front of the asperity exhibited positive vertical deformations whereas parts of the buttress behind the asperity experienced compressive strain (with magnitudes increasing with the distance from the asperity), implying rotation of the dam. Near the failure load for these models, the only interface elements which were in contact were those located on the loaded side of the asperity (i.e. upstream side) and at the toe of the dam.

While the study only implemented the structural integrity of the dam as a criterion for failure, separation between the front plate and the foundation, potentially causing seepage, was also considered as a criterion for failure. For some models in this study, a small gap (often less than 0.05 mm) appeared between the front plate and the foundation. However, it is difficult to establish a failure criterion with respect to the separation between the front plate and

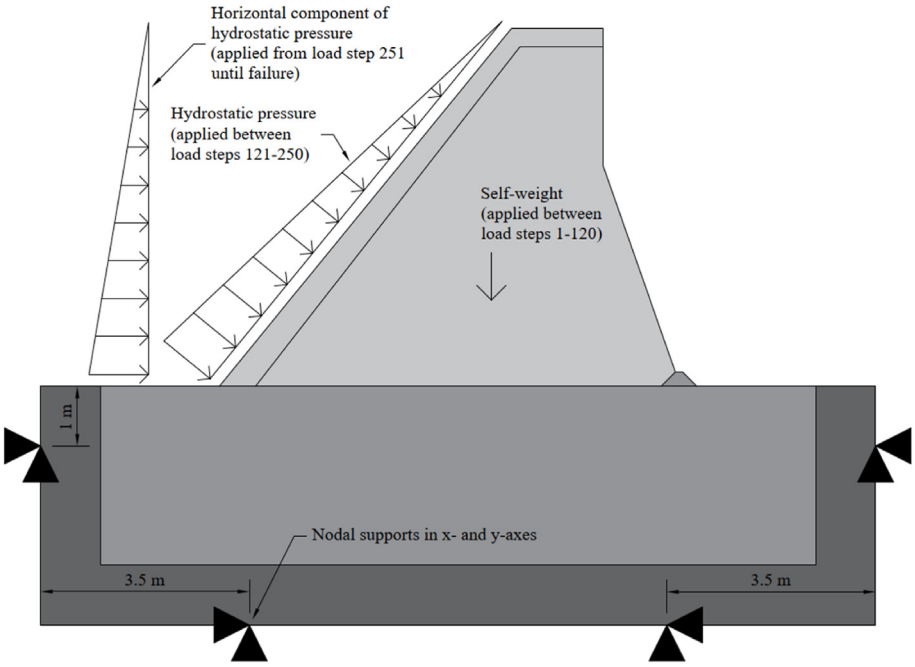

Fig. 5. Overview of loads and supports applied in the FE models.

the foundation due to the difficulty in quantifying the water seepage with regard to the size of the opening. This is partly due to FEA models being idealisations and probably not containing, e.g. cut-off trenches, which could influence seepage in case of separation between the front plate and foundation. However, any separation of the front plate and foundation in the models occurred during the load steps immediately before or at a violation of the failure criteria given in Section 3.4. Thus, a failure criterion for the separation of the front plate and the foundation would only slightly decrease the failure load for some models.

Cracks were observed in the asperity for all models (even for the models with a low asperity inclination). The cracks initiated at the base of the asperity on the loaded side and propagated further along the asperity's base (without being the cause of failure) with increasing inclination of the asperity. The cause of these cracks is due to the maximum principal tensile stresses, that arise from the force transfer between the dam and asperity, exceeding the tensile strength of the rock. Furthermore, compressive stress concentration at the loaded side of the asperity was observed in all the models.

4.1. Sliding failure

A model was considered to fail by sliding if the horizontal displacement was close to uniform over the base of the dam and only varied slightly over the dam's height as seen in Fig. 6a. Note that the displacements of the dam in Fig. 6a are magnified for greater visibility. Fig. 6b shows the shear stresses in the interface, for the same model, at various load steps. Furthermore, for a model to be considered to have failed by sliding, crack lengths and widths had to be small, with no indication of impairing the structural integrity. A total of 28 models (27 models with the asperity and the reference model) were considered to have failed by sliding. The reference sample and all the models with an asperity inclination of 15° and 20° failed as such, regardless of the asperity's location or the foundation strength. Furthermore, for the models in which the asperity was located at 100% (at the toe of the dam) and with an

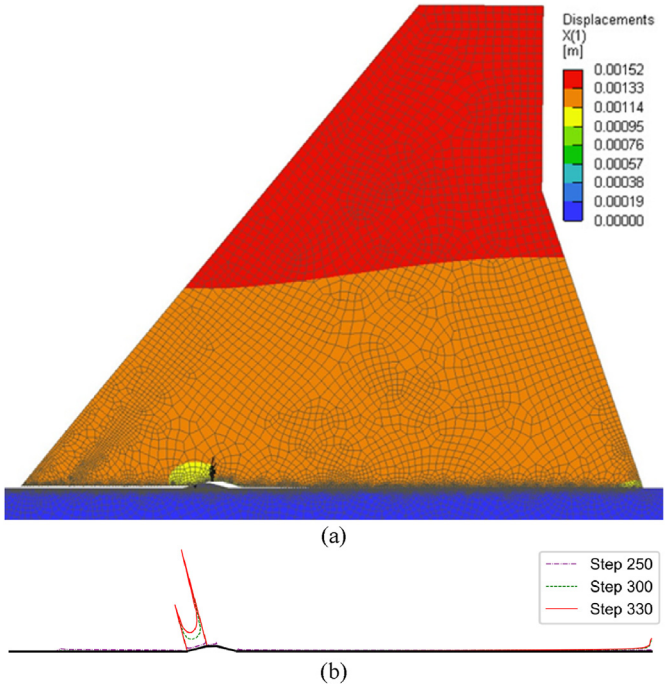

Fig. 6. (a) Horizontal displacement of a model considered to have failed by sliding. The asperity in the model had an inclination of 15° and was located at 25% of the dam's length from the front plate, and (b) shear stress plot at the interface at different load steps (full design hydrostatic load is applied at load step 250, see Section 3.4).

inclination of 25°, the failure obtained was also sliding, which was unique for models with an asperity inclination of 25°.

The foundation's (i.e. asperity and rock foundation) strength had no impact on the load capacity of the models which experienced sliding as the failure load was similar, regardless of the foundation strength.

4.2. Failure of the buttress

Failure of the buttress was deemed to have occurred when a crack emerged in the buttress and rapidly propagated towards the front plate near the failure load. The crack emerged in the concrete at the top of the asperity and progressed towards the front plate, causing a noticeable difference in the displacement in front and behind the asperity as seen in Fig. 7a. Note that the displacements of the dam in Fig. 7a are magnified for greater visibility. Fig. 7b shows the shear stresses in the interface, for the same model, at various load steps.

A total of 32 models out of 85 were considered to have failed due to failure (i.e. rupture) of the buttress. It was observed that the location of the asperity and the foundation's strength significantly influences the failure mode and shear strength. None of the samples with an asperity at the toe failed due to rupture of the buttress, while asperities with inclinations above 25° located at 25% of the dam's length always failed due to rupture of the buttress. Furthermore, for models with a foundation rock strength of 150 MPa, all asperities having an inclination above 25° at 25%, 50% and 75% failed by rupture of the buttress.

The foundation strength should not have an influence on the load capacity for models that failed due to rupture of the buttress. However, the failure load differed slightly for some models with identical geometries but with different foundation strengths. This could be attributed to slightly different crack development and propagation in the asperity leading to stress redistributions and the difference in modulus of elasticity for the foundation material models.

4.3. Failure of the asperity

Models were considered to have failed due to shearing of the asperity if the crack in the asperity base rapidly propagated when the models neared the failure load. Shearing of the asperity also caused a distinct horizontal displacement pattern as displacements grew with increasing distance from the toe, as seen in Fig. 8a. Note that the displacements of the dam in Fig. 8a are magnified for greater visibility. Fig. 8b shows the shear stresses in the interface, for the same model, at various load steps. The crack started at the bottom of the loaded side of the asperity and progressed throughout the base of the asperity.

A total of 25 models out of 85 failed by failure in the asperity. All the models with asperity inclinations above 25° and with foundation rock of 50 MPa and at the 50%, 75% and 100% locations (relative to the dam's length from the front plate) failed by failure in the asperity. All models with asperity inclinations above 30° and located at the toe of the dam failed by shearing of the asperity.

Notably, the load capacity for the models which experienced failure in the asperity had the highest load capacity of all models, as seen in Figs. 9 and 10. This is explained by the fact that the dam is reliant on the normal force transfer through the interface of the asperity for its stability.

4.4. Model load capacities

The load capacities of all models are given in Fig. 9, which shows the horizontal load capacity for the given failure mode versus the location of the asperity along the concrete-rock interface and the asperity's inclination. The figure also contains a horizontal dashed line which symbolises the load capacity of the reference model

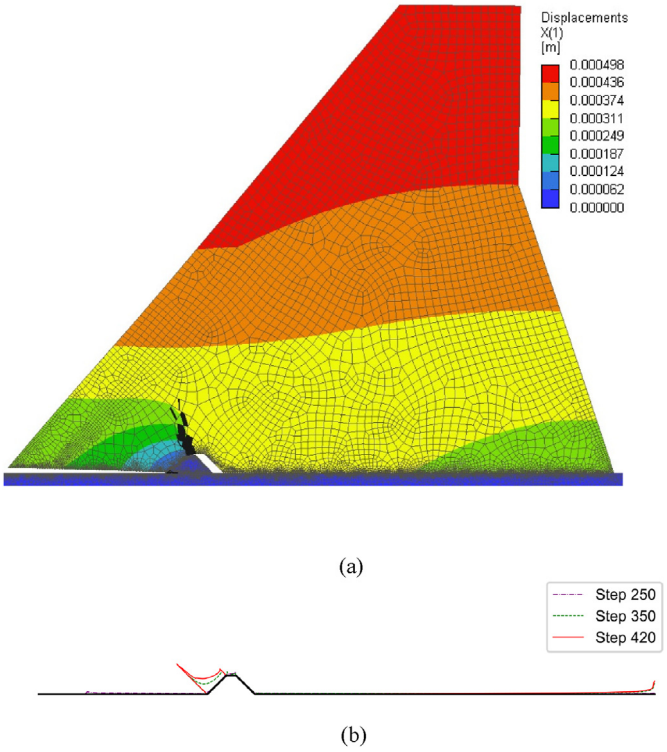

Fig. 7. (a) Horizontal displacement of a model considered to have failed by rupture of the buttress. The asperity in the model had an inclination of 45° and was located at 25% of the dam's length from the front plate, and (b) shear stress plot at the interface at different load steps (full design hydrostatic load is applied at load step 250, see Section 3.4).

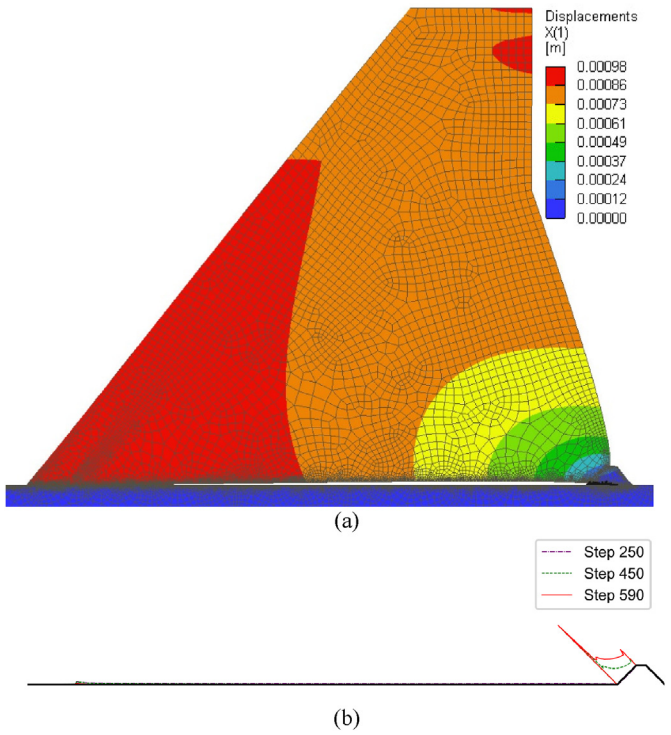

Fig. 8. (a) Horizontal displacement of a model considered to have failed due to failure in the asperity. The asperity in the model had an inclination of 45° and was located at the toe of the dam (100% of the dam's length from the front plate). (b) Shear stress plot at the interface at different load steps (full design hydrostatic load is applied at load step 250, see Section 3.4).

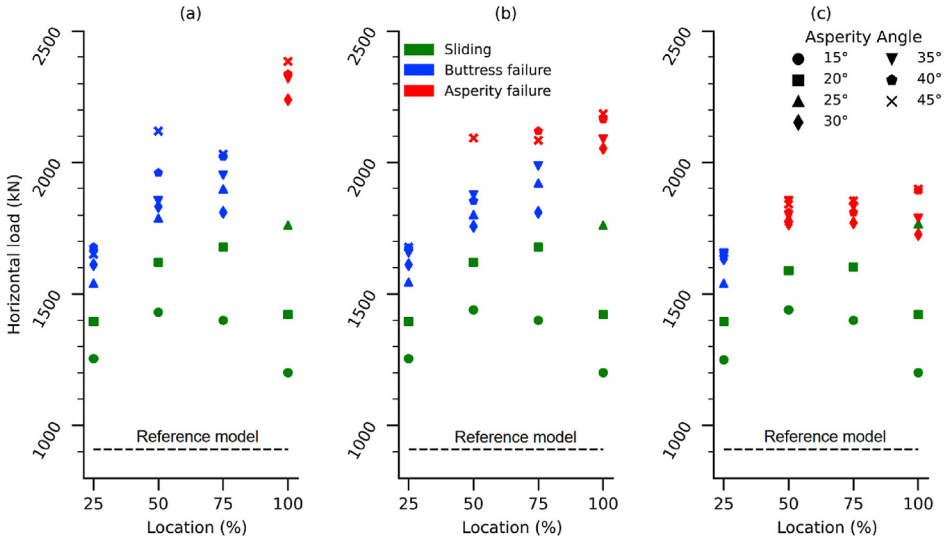

Fig. 9. Calculated shear strengths from FE model with compressive strength of (a) 150 MPa, (b) 100 MPa, and (c) 50 MPa for the foundation.

Rock strength (MPa)	Location (%)	Load at failure for each model (kN), in parenthesis ratio of load at failure of the model to load at failure of reference model													
		Inclination of asperity = 15°		Inclination of asperity = 20°		Inclination of asperity = 25°		Inclination of asperity = 30°		Inclination of asperity = 35°		Inclination of asperity = 40°		Inclination of asperity = 45°	
150	25	1254	(1.4)	1395	(1.5)	1541	(1.7)	1611	(1.8)	1656	(1.8)	1678	(1.8)	1651	(1.8)
	50	1430	(1.6)	1620	(1.8)	1788	(2.0)	1832	(2.0)	1854	(2.0)	1960	(2.2)	2119	(2.3)
	75	1400	(1.5)	1678	(1.8)	1898	(2.1)	1810	(2.0)	1951	(2.1)	2022	(2.2)	2031	(2.2)
	100	1201	(1.3)	1422	(1.6)	1762	(1.9	2238	(2.5)	2318	(2.5)	2336	(2.6)	2384	(2.6)
100	25	1254	(1.4)	1395	(1.5)	1545	(1.7)	1611	(1.8)	1656	(1.8)	1673	(1.8)	1678	(1.8)
	50	1439	(1.6)	1620	(1.8)	1801	(2.0)	1757	(1.9)	1876	(2.1)	1854	(2.0)	2093	(2.3)
	75	1400	(1.5)	1678	(1.8)	1921	(2.1)	1810	(2.0)	1987	(2.2)	2119	(2.3)	2084	(2.3)
	100	1201	(1.3)	1422	(1.6)	1762	(1.9)	2053	(2.3)	2088	(2.3)	2163	(2.4)	2185	(2.4)
50	25	1249	(1.4)	1395	(1.5)	1541	(1.7)	1634	(1.8)	1656	(1.8)	1656	(1.8)	1656	(1.8)
	50	1439	(1.6)	1589	(1.7)	1788	(2.0)	1766	(1.9)	1854	(2.0)	1810	(2.0)	1841	(2.0)
	75	1400	(1.5)	1603	(1.8)	1854	(2.0)	1770	(1.9)	1832	(2.0)	1810	(2.0)	1854	(2.0)
	100	1201	(1.3)	1422	(1.6)	1766	(1.9)	1726	(1.9)	1788	(2.0)	1894	(2.1)	1898	(2.1)
	Colour code		Sliding						Reference model	909					
			Failure in buttress												
			Shearing of asperity												

Fig. 10. Horizontal load at failure for all models (Load capacity in relation to the reference model in parenthesis).

(without an asperity in the concrete-rock interface). The reference model failed by sliding along the interface at a total horizontal load of 909 kN, which coincides with the load capacity given from analytical rigid body methods when using the MC failure criterion without cohesion, commonly prescribed by dam design guidelines (NVE, 2005; USACE, 1976; CFBR, 2012).

Furthermore, Fig. 10 also shows the load capacity of the models as well as their ratios (in parentheses) with regards to the load capacity of the reference model.

5. Analysis and discussion

5.1. Influence of inclination of asperity

Based on the results of the study, the inclination of an asperity has a significant impact on the developing failure mechanism. For asperity inclinations above 20°, the dam is likely to fail by shearing of the asperity or rupture of the buttress, with the exception of when the asperity is located at the toe. In contrast, sliding is to be expected for asperities with inclinations of 20° and below. Furthermore, the results imply that the inclination of the asperity also influences the capacity of a dam for any given failure mode, judging by the slight trend of higher capacities, in similar failure modes, for models with larger asperity inclinations. However, based on the results of this study, the ability to alter the failure mode increased the load capacity the most.

From the results of the models, the explanation as to why the asperity inclination has an impact on the failure mode and the capacity is due to the force transfer between the dam and the asperity. When the load increases, the principal stress axes in the asperity and dam, near the interface, rotate where the minimum principal stress becomes increasingly more horizontal.

Consequently, as the principal maximum stress axis becomes increasingly misaligned with the asperity's upstream face, a larger portion of the force is transferred by shear in the interface at the asperity, which explains why the asperity impacts the failure mode.

For all failure modes, the shear stress at the asperities' interfaces was non-uniform and had the greatest magnitudes at the top and base of the asperity. As these shear stress concentrations exceed the shear strength, slight displacement along the interface ensues and redistribution of stresses occurs. As the load further increases, this mechanism repeats and is the likely explanation for the inclination's impact on the capacity for the models which slide. Furthermore, as the shear stress increases and the principal maximum stress axis rotates towards the vertical axis, and further misaligns with the asperity's upstream face, larger tensile stresses arise in the asperity. These tensile stresses eventually cause cracks and crack propagation in the base of the asperity and are likely the cause as to why the models which failed by shearing of the asperity had higher capacity for larger inclinations.

5.2. Influence on location of asperity

Models with an asperity inclination of 25° or less, which failed by sliding, displayed a trend of having a greater load capacity when the asperity was located at 50% or 75% of the dam's length, in contrast to 25% or 100%. This scenario was accentuated with larger inclinations of the asperity.

For these models, the length of the interface over which forces were transferred shrank with the increasing loads. Nearing failure, the only parts of the interface in contact were at the asperity, the toe, and heel of the dam. This implies that the dam body deformed slightly near the asperity, causing the interface to lose contact in parts in between the heel and the asperity, and the toe and asperity. Furthermore, with the increase in load, upwards vertical displacement was seen at the heel and compressive strains at the toe, implying slight rotation of the models combined with sliding over the asperity (visible in Figs. 6 and 7). As the interface stress at the heel decreased and neared zero, the stresses in the dam toe grew exponentially. This was subsequently followed by failure of the models. Models with the asperity located at the 50% and 75% showed larger compressive normal stresses in the heel and required more rotation for these stresses to diminish, resulting in a higher load capacity. For the model with the asperity located at 100% (i.e. the toe), this failure mechanism was not seen. Instead, these models relied almost solely on force transfer through the interface at the asperity at the later stages of the analysis.

Models which failed by shearing of the asperity did not exhibit the behaviour discussed above. The reason is that the asperity failed before this failure mechanism could develop, as the inclination of the asperity was sufficiently steep, and these models were therefore not reliant on the location of the asperity.

For models which experienced failure of the buttress, the load capacity was heavily influenced by the location of the asperity. This is simply explained by the fact that the discontinuity region is located further away from the upstream face of the dam for an increasing distance of the asperity to the dam heel. This allows for stress concentrations to be redistributed throughout a larger portion of the buttress.

5.3. Influence of rock strength

When the asperity was located sufficiently far towards the downstream side of the concrete-rock interface and was appropriately steep, asperity failure was induced due to interlocking between the foundation and the dam. As can be seen in Fig. 9, the load capacity of the models which experienced asperity failure was relatively constant between the models with the same rock strength, but drastically differed between those with different rock strengths. This implies that the rock strength is the governing parameter for the load capacity in this type of failure mode. More precisely, the tensile strength of the rock is the governing parameter as failure initiates when the principal stresses exceed the tensile strength of the rock material.

5.4. Implications for dam safety

The results obtained from the FE models showed that the horizontal load capacity of the dam is 30%–160% higher than the capacity of the reference model that did not include a large-scale asperity in the concrete-rock interface (equivalent to assessment by analytical rigid body methods). This corresponds to an increase of water level of 1 m–3.8 m over the crest of the dam in this study (with a height of 6 m). Furthermore, the results show that asperities with a length of at least 10% of the dam's height and with an inclination of at least 30° act like shear keys, by preventing movement. The asperity, granted that it has an appropriate size, may therefore prevent sliding along the concrete-rock interface and increase the horizontal load capacity of the dam. Consequently, the likelihood of a failure occurring in the concrete-rock interface decreases for interfaces that contain large-scale asperities. For such concrete-rock interfaces, due to the interface's increased capacity to transfer horizontal loads, the likelihood of failure in the foundation (e.g. sliding along a persistent rock joint or asperity failure) or in the dam body being governing increases. Therefore, in practice, the foundation of a dam should be modelled carefully based on the geological conditions to not prevent or overlook any potential failures in the foundation to develop. Furthermore, it should be verified that the large-scale asperities cannot slide along a shallow persistent rock joint which could otherwise negate their beneficial effect.

Numerous concrete dams were constructed to meet lower safety requirements than those in practice today (ICOLD, 2004; Sas et al., 2021). Consequently, many of these dams do not fulfil the safety requirements according to current guidelines and regulatory rules when assessed using analytical rigid body methods, resulting in costly strengthening of dams. However, by accounting for the positive influence of large-scale asperities on the load capacity of a dam, e.g. through FEA, many such dams could potentially be proven to fulfil the current requirements for safety.

It should be remembered that a conservative estimate for the tensile strength of the foundation rock was used in this study. As the tensile strength of the asperity appears to be the governing factor in the strength of the model for samples failing in asperity, the strength of the asperity may have been underestimated in the study.

While interpreting the results, it should be noted that the study did not consider pore pressure. The dam in the models displaced along the concrete-rock interface, although very slightly, which potentially could result in an increase of pore pressure and loss of serviceability. However, such failures were not addressed in this study. Furthermore, in an actual dam, multiple asperities could be present in the concrete-rock interface. Further studies are required to understand the behaviour of multiple asperities and any potential interaction between them. Additionally, the study was based on the assumption of intact foundation rock and direct application of the results of this study to different geological conditions should therefore be undertaken with caution.

6. Conclusions

The objective of this parametric study was to employ finite

element analysis to investigate the influence of foundation strength and an asperity's inclination and location in the concrete-rock interface on the load capacity and failure mode of a buttress dam.

The results show that interlocking between the asperity and dam can be expected for asperity inclinations of 30° and larger, where the interlocking results in either failure of the buttress or asperity. For models that experienced interlocking, the location of the asperity and the tensile strength of the foundation material determined whether the buttress or large-scale asperity failed. For lower asperity inclinations, 25° or smaller, the failure mode was predominantly sliding over the asperity.

Failure in the buttress was heavily influenced by the location of the asperity in the concrete-rock interface as a higher load capacity was seen for models in which the asperity was located closer to the toe of the dam (the point in the dam furthest downstream). The location of the asperity did not have a significant influence on the capacity for the models that failed by shearing of the asperity. For models which experienced sliding failure, the highest load capacity was seen when the asperity was located near the centre of the dam.

The models which experienced failure of the asperity generally displayed the highest load capacity, followed by the models that failed by rupture of the buttress. The lowest horizontal load capacity was attained from the model where the asperity was located at the toe of the dam and had the lowest inclination implemented in the study (15°), for which a sliding failure was obtained. With reference to the horizontal load capacity given for the model without an asperity (the reference model), models that failed by sliding had a 30%–90% higher capacity, depending on the location and inclination of the asperity. Models that failed by rupture of the buttress had an increase of 70%–130%, mainly determined by the location of the asperity. For the models in which the asperity failed, the horizontal load capacity was 90%–160% higher than that of the reference model, depending mainly on the tensile strength of the rock. Regardless of the failure mode, large-scale asperities in the rock concrete interface may have a significant influence on the load capacity of dams. Consequently, the load capacity of a dam may be underestimated when employing analytical rigid body methods given in the current regulatory rules and guidelines, as they do not consider the favourable influence of large-scale asperities.

Declaration of competing interest

The authors declare that they have no known competing financial interests or personal relationships that could have appeared to influence the work reported in this paper.

Acknowledgments

The authors are grateful to the various funding agencies: the Research Council of Norway (Grant No. 244029) funding the project 'Stable dams', FORMAS (Grant No. 2019–01236) funding the project 'Improved safety assessment of concrete dams', and SVC (Grant No. VKU32019) funding the project 'Safe dams', that supported the development of the research presented in this article. The authors would also like to thank Mr. Bård Arntsen at ICEMATE AS, Narvik for his support in this research.

References

ANCOLD, 1991. Guidelines on Design Criteria for Concrete Gravity Dams, Australian National Committee on Large Dams.

Andjelkovic, V., Pavlovic, N., Lazarevic, Z., Nedovic, V., 2015. Modelling of shear characteristics at the concrete–rock mass interface. Int. J. Rock Mech. Min. Sci. 76, 222–236.

Asadi, M.S., Rasouli, V., Barla, G., 2013. A laboratory shear cell used for simulation of shear strength and asperity degradation of rough rock fractures. Rock Mech. Rock Eng. 46, 683–699.

Bandis, S., Lumsden, A.C., Barton, N., 1981. Experimental studies of scale effects on the shear behaviour of rock joints. Int. J. Rock Mech. Min. Sci. 18, 1–21.

Bista, D., Sas, G., Johansson, F., Lia, L., 2020. Influence of location of large-scale asperity on shear strength of concrete-rock interface under eccentric load. J. Rock Mech. Geotech. Eng. 12 (3), 449–460.

Briševac, Z., Kujundžić, T., Čajić, S., 2015. Current cognition of rock tensile strength testing by Brazilian test. Rudarsko-Geolosko-Naftni Zb. 30, 101–128.

Červenka, V., Jendele, L., Červenka, J., 2021. ATENA Program Documentation, vol. 1. Theory, Prague, Czech Republic.

CFBR, Comité Français des Barrages et Réservoirs, 2012. Recommendations for the Justification of the Stability of Gravity Dams.

Enzell, J., 2023. Toward Realistic Failure Evaluations for Concrete Buttress Dams. Licentiate Thesis. KTH Royal Institute of Technology, Stockholm, Sweden.

EPRI, Electric Power Research Institute, 1992. Uplift pressures, shear strengths and tensile strengths for stability analysis of concrete gravity dams. Stone and Webster Eng. Corp. 1, 304. Denver, Colorado.

EN 1992-1-1, 2004. Eurocode 2: Design of Concrete Structures-Part 1-1. General Rules and Rules for Buildings.

FERC, 2016. Engineering Guidelines for the Evaluation of Hydropower Projects. Chapter 3: Gravity Dams, Federal Energy Regulatory Commission.

Grasselli, G., 2001. Shear strength of rock joints based on quantified surface description. Ecole Polytechnique Federale De Lausanne. EPFL), Lausanne, Switzerland. PhD Thesis.

Grasselli, G., 2006. Manuel rocha medal recipient shear strength of rock joints based on quantified surface description. Rock Mech. Rock Eng. 39, 295–314.

Hencher, S.R., Toy, J.P., Lumsden, A.C., 1993. Scale dependent shear strength of rock joints. In: Scale Effects in Rock Masses, 93. first ed. CRC Press, pp. 233–240.

Hoek, E., Brown, E.T., 1997. Practical estimates of rock mass strength. Int. J. Rock Mech. Min. Sci. 34, 1165–1186.

ICOLD, 2004. Sliding safety of existing gravity dams - Final report. https://britishdams.org/assets/documents/conferences/2004/reports/sliding.pdf.

Johansson, F., Stille, H., 2014. A conceptual model for the peak shear strength of fresh and unweathered rock joints. Int. J. Rock Mech. Min. Sci. 69, 31–38.

Kodikara, J.K., Johnston, I.W., 1994. Shear behaviour of irregular triangular rock-concrete joints. Int. J. Rock Mech. Min. Sci. Geomech. 31, 313–322.

Liahagen, S.A., Lia, L., Jørstad, O., Sas, G., 2012. Stabilitet Av Betongdammer - Ruhetens Påvirkning På Skjærkapasiteten Mellom Betong Og Berg. Norwegian University of Science and Technology (NTNU), Trondheim, Norway. Master's Thesis.

NVE, 2005. Guidelines for Concrete Dams. Norges Vassdrags-Og Energidirektorat, Norwegian Water Resources and Energy Directorate. Oslo, Norway.

Patton, F.D., 1966. Multiple modes of shear failure in rock. In: Proceedings of the 1st Int. Congr. Rock Mech..

Perras, M.A., Diederichs, M.S., 2014. A review of the tensile strength of rock: concepts and testing. Geotech. Geol. Eng. 32, 525–546.

Pryl, D., Červenka, J., 2018. ATENA Program Documentation Part 11 - Trouble-shooting Manual. Prague, Czech Republic.

Sas, G., Bretas, E.M., Lia, L., 2015. Advanced Sliding Assessment of Målset Dam: Tests and Numerical Analysis of Unbonded Joints. Stavanger Congress 2015, Stavanger, Norway.

Sas, G., Popescu, C., Bista, D., Seger, A., Arntsen, B., Johansson, F., et al., 2021. Influence of large-scale asperities on the shear strength of concrete-rock interface of small buttress dams. Eng. Struct. 245.

USACE, 1976. Stability Analysis of Concrete Structures: EM 1110-2-2100. US Army Corps of Engineers, Washington D.C., USA.

Westberg Wilde, M., Johansson, F., 2016. Probablilistic Model Code for Concrete Dams: Report:292. Energiforsk, Stockholm, Sweden.

Wu, X., Yang, P., Chen, J., 2018. The strain softening model of rock damage under compression and tension. Int. J. Eng. Model. 31 (3).

Zhang, Y., Lu, W., Chen, M., Yan, P., Hu, Y., 2013. Dam foundation excavation techniques in China: a review. J. Rock Mech. Geotech. Eng. 5, 460–467.

Zhang, X., Jiang, Q., Chen, N., Wei, W., Feng, X., 2016. Laboratory investigation on shear behavior of rock joints and a new peak shear strength criterion. Rock Mech. Rock Eng. 49, 3495–3512.

Dipen is a civil engineer at Sweco, Norway and a PhD candidate at the Norwegian University of Science and Technology (NTNU) in Trondheim, Norway. He has extensive experience in the hydropower and research industry, working on various projects related to dams and renewable energy. His research interests are in dam engineering, with a special focus on the concrete dams.